Journal of Neurology & Experimental Neuroscience

https://doi.org/10.17756/jnen.2022-096

Research Article

Open Access

A Characterization of Epileptiform Activity Associated with TAU Seeding and Amyloid Pathology in the APPK-M670/671NL.PS1/L166P and APP-KI Animal Models

Sean Tok [1,2], Dries Crauwels[1] and Wilhelmus Drinkenburg[1,2*]

[1]*Department of Neuroscience, Janssen Research & Development, Janssen Pharmaceutica NV, Turnhoutseweg, Beerse, Belgium*

[2]*Groningen Institute for Evolutionary Life Sciences, Faculty of Science and Engineering, University of Groningen, Netherlands*

***Correspondence to:**
Wilhelmus Drinkenburg,
Department of Neuroscience, Janssen Research & Development, Janssen Pharmaceutica NV, Turnhoutseweg, Beerse, Belgium
Tel: +3247046 91 04
E-mail: wdrinken@its.jnj.com

Received: July 11, 2022
Accepted: September 19, 2022
Published: September 22, 2022

Citation: Tok S, Crauwels D, Drinkenburg W. 2022. A Characterization of Epileptiform Activity Associated with TAU Seeding and Amyloid Pathology in the APPKM670/671NL.PS1/L166P and APP-KI Animal Models. *J Neurol Exp Neurosci* 8(2): 18-31.

Copyright: © 2022. Tok et al. This is an Open Access article distributed under the terms of the Creative Commons Attribution 4.0 International License (CC-BY) (CC-BY) (http://creativecommons.org/licenses/by/4.0)which permits commercial use, including reproduction, adaptation, and distribution of the article provided the original author and source are credited.

Published by United Scientific Group

Abstract

Patients suffering from Alzheimer's disease (AD) exhibit an increased risk for developing seizures and epileptiform activity, especially at the later stages of the disease. At earlier stages of the disease, epileptiform activity is thought to be a manifestation of network hyperexcitability. Animal models of AD pathology have been suggested to exhibit similar epileptiform activity, but it remains unclear what the pathological correlates are. However, confounds associated with the presence of amyloid pathology in these animal models such as protein overexpression may influence the development of epileptiform activity. This study aimed to determine the pathological correlates of epileptiform activity in the APPKM670/671NL.PS1/L166P and APP-Knock in animal models, which do and do not exhibit protein overexpression respectively. These mice also underwent tau seeding using human-derived seeding material, and were followed across a period of 5 months after injection. We report that while APP.PS1 animals exhibit clear indications of epileptiform activity and network hyperexcitability in behavioural states of inactivity, APP-KI animals failed to show similar signs. APP.PS1 animals exhibited significantly more epileptiform activity that reduced with age, which appeared to be counteracted by tau seeding, compared to buffer and wild-type controls. Interestingly, tau seeding immediately elicited acute epileptiform activity in younger APP-KI animals, but not APP.PS1 animals or older APP-KI animals. Longitudinal effects of tau pathology were not associated with significantly increased epileptiform activity. These findings suggest that epileptiform activity in APP.PS1 animals may be associated with factors other than amyloid plaque pathology and that tau-seeding induces the development of epileptiform activity.

Keywords

Epileptiform activity, Seizures, Alzheimer's disease, Animal models, Amyloid plaques, Tau pathology, Protein overexpression, Tau seeding

Introduction

Patients suffering from Alzheimer's Disease (AD) exhibit an increased risk for developing seizures and epileptiform activity over the course of the disease [1]. Previous studies have reported that unprovoked seizures may occur in 0.5-64% of patients suffering from AD, and are more frequent in patients that exhibit the familial, early-onset form of AD. This also suggests that disease severity as reflected by the earlier onset, may be associated with the development of seizure-related activity. While certain forms of epileptiform seizures manifest physically as convulsions or episodes of absence (i.e., absence seizures), recent reports have suggested a host of other subtle epileptiform activity that accompany AD, but

may go undetected [2]. Furthermore, the presence of seizures have also been correlated with faster cognitive decline [1, 3], highlighting the functional and clinical relevance of epileptiform activity.

The concept of Network hyperexcitability (NH) is commonly associated with the presence and development of seizures and hypersynchronous activity in neural networks [4], and has been suggested to be a prodromal indicator of AD [2, 5, 6] due to its early temporal onset. Several putative indications of hyperexcitability such as the presence of increased cortical excitability, hippocampal hyperactivity, aberrant default mode network activation, and development of seizures and epileptiform activity are thought to be present in the early stages of the disease [5]. Thus, the presence of NH in the form of seizures or others, may be a key tool in detecting patients at the early stages of the disease, where therapeutic intervention may be more efficacious.

Animal models used to study AD that exhibit amyloid pathology, generally showcase hyperexcitability-related behavior in the form of their propensity to exhibit unprovoked seizures [7], increased susceptibility to pharmacologically [8] and audiogenic seizures [9] as well as epileptiform-like activity [10, 11]. This effect also does not appear to be limited to a single amyloid animal model but appears to be a common trait across multiple amyloid pathology models [8-10, 12], indicating that seizures may be strongly associated with amyloid pathology.

However, recent evidence has suggested that animal models of amyloid pathology may exhibit epileptiform-like and seizure-like activity that may not be directly associated with the presence of amyloid pathology. In one such study, Born and colleagues noted that the presence of epileptiform activity was linked to the expression levels of the APP protein, rather than the presence of amyloid plaque pathology [13]. Other reports have indicated that even just the expression of wild-type human APP significantly alters the neurophysiology of the animal in the absence of amyloid plaque pathology [14]. Another study has demonstrated that the overexpression of wild-type human APP is linked to the reduction of gamma-Aminobutyric acid (GABA) levels in a mouse model [15], a key player regulating the inhibition of neural networks. These reports prompt a closer evaluation of the presence of seizure and epileptiform activity by controlling for the presence of overexpression-associated side effects by using newer animal models, such as the APP knock-in animal mouse model family [16].

Some of the seizure-like and epileptiform activity in animal models of amyloid pathology have been reported to resemble spike-wave-discharges, interictal spikes, as well as unprovoked electroencephalographic seizures [8, 10].

Thus, this study sought to quantify and compare the presence of epileptiform-like activity between APP.PS1 and APP-KI animal models using an epileptiform detection workflow as seen in (Figure 1a). In this present study, some of the more prominently described epileptiform-like activity, such as single spikes (Figure 1b), poly spikes (Figure 1c), as well as electroencephalographic seizures (Figure 1d) were noted to occur in APP.PS1 and APP-KI animals and could be quantified, allowing for a direct comparison.

This present study investigated and compared three forms of NH activity present in the APP.PS1 and APP-KI animal models, as well as control groups from two studies that were previously carried out in terms of hisopathological and neurophysiological characterization [17, 18]. These studies were previously carried out with a focus on understanding the neurophysiological effects of pathology, but did not focus on NH-related aspects. Thus in this present study, these datasets were used to investigated the presence of interictal-like single spikes and poly-spike phenomena, which are thought to reflect subclinical NH activity, as well as electroencephalographic seizure-like activity as described by [19, 20].

This was carried out in the presence of tau seeding, which resulted in prominent AT8-positive tau pathology, as observed in previous studies. We sought to understand if NH in the form of seizure-like and epileptiform-like activity could be attributed to the presence and amount of pathology. In addition, we sought to understand if any of these phenomena could be attributable to APP protein overexpression, rather than pathology. In this study, we used APP.PS1 animals, which are reported to express APP at approximated 3-fold higher than wild-type controls [21].

Materials and Methods

Animal cohorts and usage

Data were obtained from heterozygous APP KM670/671NL.PS1/L166P (B6.Cg-Tg(Thy1-APPSwe,Thy1-PSEN1*L166P)21Jckr) mice, line 21, on the C57BL/6 background [21] and Wild-type C57BL6 littermates as well as homozygous APPNL-G-F/NL-G-F and APPNL/NL mice on the C57BL/6 background [16]. Animal housing conditions, diet, light-dark cycles, except for food restriction were identical to the conditions listed in Jacob et al. [22]. Animals were given ad libitum access to food (SAFE A05 diet, SAFE DIETS) and water. Animals were also equally balanced for sex as much as possible.

Animals used in the analysis of this study were previously used to study the histopathological and neurophysiological characteristics of the interaction between amyloid and tau pathology. As such, the datasets used for epileptiform analysis in this study are exactly the same as those in Tok et al. [17, 18]. For representative histological images of the animals, please refer to supplementary figure 3. For the purposes of clarity in this study, APP.PS1 animals that received tau injections are referred to as APP.PS1-tau animals, and wild-type animals as WT-tau, along with their respective buffer-injected control groups (i.e., APP.PS1-Buffer and WT-Buffer). APP-KI animals will be referred to as NL-G-F and NL animals, with their respective injection conditions (i.e., NL-G-F-Tau, NL-G-F-buffer, NL-Tau and NL-Buffer). For each genotype-treatment group (e.g. NL-G-F-Tau), 16 animals (8 male/8 female) were in each group at the start of the study, while it should be noted that limited attrition occurred across time points.

All *in vivo* and *in vitro* studies were performed in strict accordance with the guidelines of the Association for Assessment and Accreditation of Laboratory Animal Care International (AAALAC) and with the European Council Directive

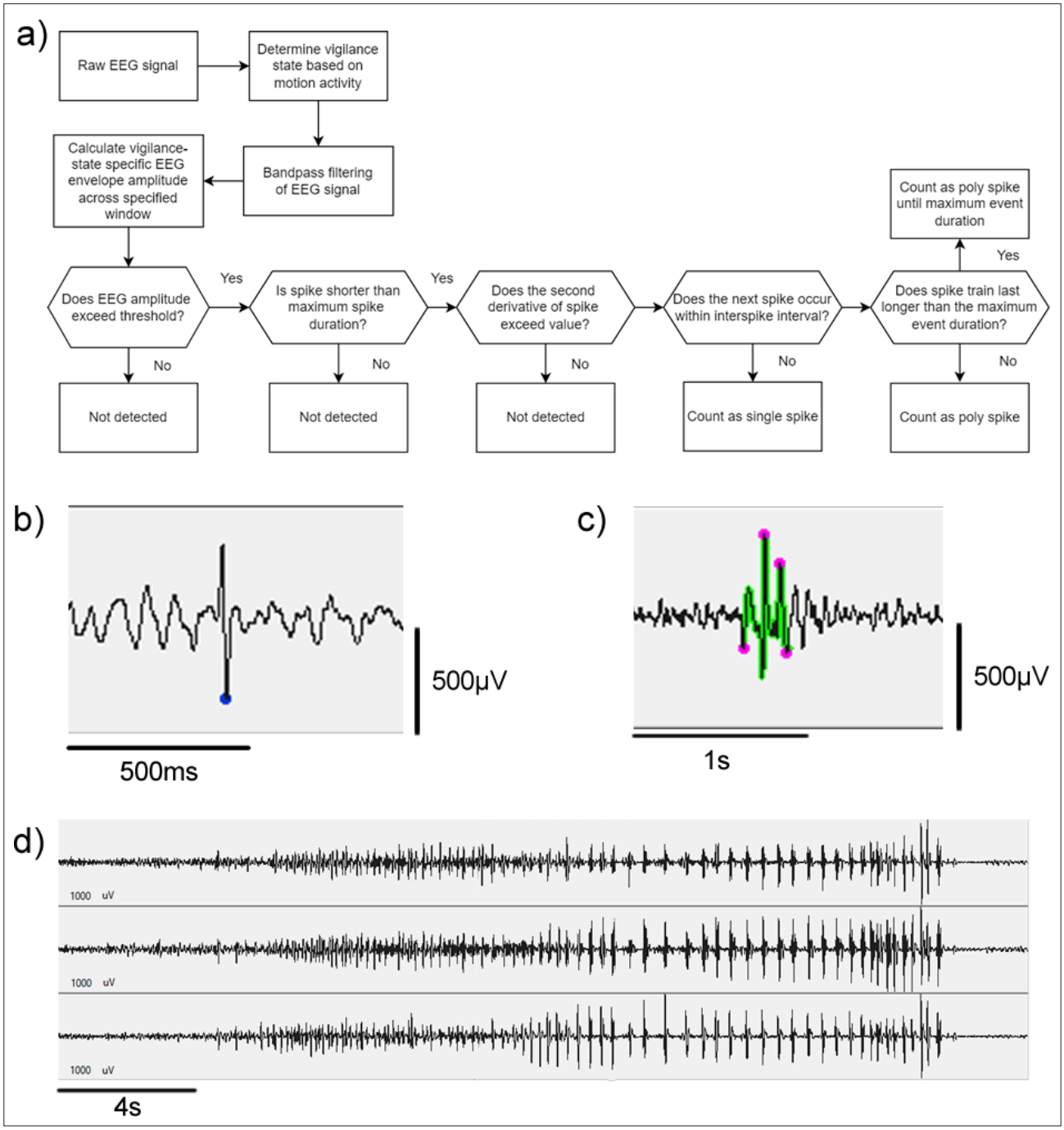


Figure 1: Overview of seizure and epileptiform activity detection workflow, as well as representative examples of epileptiform activity. a) Workflow for detection of the single, poly spikes and seizure events. Seizure episodes were detected as 'poly spikes' using parameters optimized for long-lasting events. b) Representative example of a single spike detected from an APP.PS1 animal showing a positive to negative deflection lasting a short duration, with the blue dot indicating the point where the amplitude is maximally distant from the detection threshold. c) A representative example of a poly spike event detected from APP.PS1 animals, with closely-spaced spikes being detected as a contiguous event, highlighted in green and maxima and minima points highlighted with purple dots. d) Representative example of a generalized seizure episode detected from an APP-KI animal following injection of tau seeds. Top, middle and bottom traces are Hippocampal, Retrosplenial cortex and Medial entorhinal cortex recording traces respectively. The LFP evolves temporally from lower amplitude discharges that increase in amplitude and duration in between discharges, and terminates in a post-ictal-like suppression.

of 24 November 1986 (86/609/EEC) and European Ethics Committee directive (2010/63/EU) for the protection of laboratory animals. In line with Belgian governmental directives all protocols were approved by the Animal Care and Use Committee of Janssen Pharmaceutica NV.

In vitro and *ex vivo* methods

AD-tau seed purification

Human brain samples were obtained from the University of Washington brain bank as a generous gift from Virginia M.Y. Lee and John Q. Trojanowski. The use of post-mortem

brain tissues for research was approved by the University of Pennsylvania's Institutional Review Board with informed consent from patients or their families. Purification methods for the preparation of AD-Tau seeds were followed according to the protocol listed in [23] and detailed below. All methods were performed in accordance with the relevant guidelines and regulations.

Patient brain samples stored at -80 were thawed and transferred to a precooled metal cooling block. Grey matter was separated using metal forceps and was kept for subsequent extraction of seeding material. Total grey matter weight was recorded and extraction buffer was added before homogenization (QuickPrep, FastPrep-24, 4m/s, 30 s) and stored at -80.

Homogenates were thawed and centrifuged at 10,000 g for 10 mins at 4 ºC. The supernatant was separated and kept. The pellet was re-homogenized by adding 30 ml of extraction buffer per 180 ml of homogenate and re-homogenized (QuickPrep, FastPrep-24, 4m/s, 30s). This was subsequently centrifuged again at 10,000 g. 25% Sarkosyl was added to the supernatant from the first centrifugation step to a final concentration of 1% Sarkosyl in the mixture and stirred at 100 rpm, room temperature. The supernatant from the second centrifugation step was separated from the pellet and 25% Sarkosyl was added to a final concentration of 1% Sarkosyl. The two volumes of supernatants containing Sarkosyl were combined and stirred for 1.5 h at 100 rpm, room temperature and subsequently referred to as the Sarkosyl mixture.

The Sarkosyl mixture was subsequently centrifuged at 150,000 g for 75 mins at 4 ºC. The resulting supernatant was decanted, and the pellet gently rinsed with PBS 3 times. Pellets were reconstituted with PBS and vortexed at 2000 rpm for 1 minute. Another 23 ml of PBS was added and another round of centrifugation at 250,000 g, for 30 mins, at 4 degrees Celsius was performed. The supernatant was decanted, and the pellet transferred to a 2 ml Eppendorf tube, which was subsequently filled with PBS and rocked for 12-16 hours (Hoola-mixer, orbital 5rpm 15sec, reciprocal 45° 10sec, vibro 5° 5sec).

This was subsequently centrifuged at 1000 g for 1 minute at room temperature before using a 20-, 23- and 26-gauge needle and syringe consecutively to break the pellet into smaller pieces by passing the suspension through the syringes repeatedly. This mixture was sonicated (Sonotrode, Amplitude 100%, Cycle = 50% and Total watts of 200W). This was subsequently centrifuged in 1 ml ultracentrifuge tubes at 100,000 g for 30 mins at 4 ºC. The supernatant was removed and reconstituted with PBS, before repeating the same process of breaking the pellet using a 23 and 26-gauge needle. This was subsequently centrifuged at 1000 g for 1 minute at room temperature and sonicated again at the same settings.

A final centrifugation at 10,000 g was carried out for 30 mins at 4 ºC and the supernatant collected as AD-Tau seeding material, subsequently stored at -80 ºC. This was performed on brain samples from 6 different patients on different days and the purified seeds from each sample were pooled. Purified seeds from each purification, as well as the pooled sample were checked for seeding in mouse primary neurons.

In vivo methods

Surgical procedures

Surgeries were carried out when mice were 2-2.5 months old and 5-5.5 months old. Anaesthesia was induced via isoflurane inhalation (O_2, N_2O and 5% isoflurane), followed by the shaving of the fur and disinfection with Isobetadine (Meda Pharma SA, Belgium) and 70% Ethanol. Analgesics (dipidolor, 0.025 mg/kg, Xylocaine, 10%), and eye ointment (Opticorn A, EcuPhar BV, Belgium) were applied to the animal prior to insertion into a stereotactic frame. The animal was maintained under isoflurane during surgery (O_2, N_2O and 2-2.5% isoflurane), and kept at 37-38 ˚C using a heating pad. An incision was made on the skin along the sagittal plane to expose the skull, and sutures to hold the skin apart at the lateral edges of the opening. The tilt, yaw and roll of the head was adjusted for by measuring the DV differential between the bregma and lambda sutures. All differentials were corrected to within 0.05 mm prior to drilling. Drilling locations were measured relative to bregma and drilled by hand. Stainless steel screws were affixed over the left frontal and right occipital lobes to secure the implant.

Single polyamide-coated stainless-steel wire electrodes (100 µm diameter with a blunt-tip, Peira bvba, Belgium) were implanted. The dura was punctured by a hypodermic needle (PrecisionGlide, 25g, BD) at each location and implantation of electrodes were carried out with these coordinates: Medial entorhinal cortex (AP: -4.8, ML:3.25, DV:2.2), Hippocampal CA1 (AP: -2.2, ML:1.8, DV:-1.4), Retrosplenial cortex (AP: -1.75, ML: 0.5, DV: 1.0), Thalamus (AP: -0.83, ML:0.75, DV:2.75), and Reference (AP: -1.0, ML:1.2, DV:0.8), followed by the cannula (AP: -2.5, ML:2.45, DV:1.4, lateral angle of +24.5 degrees ,C315GAS-5/SPC, Plastics One). For a schematic overview of the electrode positions, please refer to supplementary figure 1a. Each electrode was fixed with dental cement (Relyx Unicem 2 cement, 3M United States) and cured using a dental light. The ground screw electrode was implanted in the skull approximately 1mm posterior to lambda. Subsequently, a multichannel connector (Nano strip connector, Omnetics, Minneapolis, USA) was connected to the electrodes and affixed using dental cement.

The skin surrounding the surgical site was sealed using veterinary glue (Vetbond, 3M United States) after either surgical procedure. Mice recovery was closely monitored until they were fully recovered (approximately ten to fourteen days).

Animal injections

Animals were injected with either AD-tau seeding material or sterile phosphate-buffered saline (PBS) buffer solution via the cannula at 3 or 6 months of age. Animals were anesthetized and mounted into the stereotactic frame as in the surgical procedure. The needle used for injections was a Hamilton 10 µl syringe mounted onto an injection robot (StereoDrive, Neurostar, Germany). The injection needle was fitted with a custom tube and locking needle adaptor for the cannula (C315IAS-5/SPCm, Plastics One Inc.). Injection speed was set as 0.2 µl per minute and a volume of 5 µl was injected, with a waiting time of 5 mins after injection. Needles

were tested for blockage by ejection of 0.1 µl of injectate before and after injection and changed once a blockage was noted. Animals were returned to home cage and monitored for 2 hours after injection.

Animal euthanasia

Animals implanted with electrodes were electro-lesioned using a stimulator (STG4002-1.6 mA, MultiChannel Systems, GmbH) while under isoflurane anaesthesia (O2, N_2O and 2-2.5% isoflurane). A detailed description of the electro-lesion settings can be found in supplementary methods M1. Representative histological images of the results of electrode burning can be seen in supplementary figure 1b. Animals were subsequently administered a dose of pentobarbital diluted in saline (120 mg/kg) and perfused with PBS mixed with heparin (10 U/mL), followed by 4% paraformaldehyde (PFA). Brains were kept overnight in 4% PFA and washed two times in PBS for 15 mins each before transferring to a solution of 0.1% sodium azide and stored at 4 °C.

Electrophysiological recording procedures

Mice were recorded in customized plexiglass chambers (modified from Med Associates Inc. Fairfax, Vermont). These Perspex boxes were placed in opaque sound attenuated chambers fitted with a small ventilation fan and a house light. The entire home cage without the cover or food tray of the animal was placed above a plastic pedestal into the box. The house light was switched on during the entire recording duration. Each recording box was controlled by K-limbic software, (Med Associates Inc. Fairfax, Vermont, version 1.20.2). A video camera (uEye CP, IDS imaging GmbH) was mounted on the top of the chamber to record animal behavior.

Electrophysiological signals were acquired using a 4-channel wireless headstage (W2100-HS4, Multi-Channel Systems GmbH) and interface board (W2100-IFB system, Multi-Channel Systems GmbH) at a sampling rate of 1000 Hz. The wireless head stages were powered by a 30 mAh battery (Wireless-B-30mAh, MultiChannel Systems GmbH). All signals recorded were referenced and grounded to the respective physical electrodes as described in the surgical procedures. Signals and battery levels (>80%) were checked prior to recording. The Multi-Channel Experimenter software (Multi-Channel Systems GmbH, version 2.14.0.19346) was used to acquire the recordings and synchronize the video acquisition, which was carried out on a separate computer running the Multi-Channel Video Control software (Multi-Channel Systems GmbH , version 2.2.0) at 25Hz. The duration of each recording session was 1 hour in length and carried out 2 hours after the start of the dark phase. Animals were returned to the home rack after each session. Animals were recorded on 3 consecutive days at the same time each day to control for circadian effects. APP.PS1 animals were recorded at 5 time points after surgical implantation: Pre-injection (4-6 hours before injection), post-injection (1 day after injection), 1 month-post-injection (30 days) 3 months-post-injection (90 days) and 5 months-post-injection (150 days). APP-KI Animals were recorded at 4 time points after surgical implantation: Pre-injection (4-6 hours before injection), post-injection (1 day after injection), 1 month-post-injection (30 days) and 5 months-post-injection (150 days). Representative EEG traces from each animal cohort can be seen in supplementary figure 2.

Animal activity level estimation

In order to assess the activity state of the animal for subsequent analysis, the video files of each recording were processed to extract movement and activity information using DeepLabCut [24]. Once the model snapshot was finalized, the model was incorporated into a custom in-house software based on LabView (National Instruments, USA) for estimating the position of the animal and determining the activity level of the animal. A detailed protocol of the video pre-processing, tracking model, analysis, and activity level estimation can be found in supplementary methods M2.

The entire duration of each recording session was divided into 4s epochs and classified as active or inactive based on whether the activity data crossed the threshold for a sufficient duration during each epoch. The classification of animal activity was a binary state of 0 (inactive) or 1 (active) with an activity threshold calculated from 30% of the peak motion displacement over the entire recording session. Epochs that crossed the activity detection threshold were considered as active epochs, and inactive for epochs that were otherwise.

EEG data preprocessing and exclusion criteria

Local Field Potential (LFP) data was acquired from the electrophysiological recordings of the animal and divided into the same time-matched 4s epochs as used for activity detection, and subsequently processed to remove noise and artefacts using MATLAB 2016a. Animals were also excluded based on noise and artefacts that could not be removed by processing. For a detailed description of the artefact and noise detection processing algorithms, as well as specific exclusion criteria, please refer to supplementary methods M3.

Detection of seizure and epileptiform activity

Following the recommendations of Jin et al. for the scoring of epileptiform activity in preclinical models of AD [25], we modelled our approach for the detection of single spikes, poly spikes and based on these recommendations. For the detection of electroencephalographic seizures, parameters were derived from clinical guidelines for seizure definitions [19, 20]. The detection of epileptiform activity was carried out using software developed in-house (Janssen Pharmaceutica NV, Belgium) to detect spikes based on several key parameters. The key parameters used for the detection of epileptiform activity were: Bandpass filtering frequencies, Spike duration, Maximum interevent interval, second derivative value of the EEG, standard deviation amplitude threshold, maximum event duration, minimum event duration, maximum number of spikes in a single event and normalization duration. For a detailed explanation of each of these parameters, please refer to supplementary methods M5. An overview of the decision flowchart of detecting epileptiform activity can be seen in figure 1a.

Poly spike events were defined as a train of single spikes occurring no more than 200 ms between the end of a single spike and the beginning of another single spike.

Due to the EEG heterogeneity across different types of epileptiform activity, a single detection algorithm would be insufficient to accurately capture the epileptiform activities of interest. As such, two detection models containing different values for key parameters were built to detect epileptiform activity: Model 1 for detecting single and poly spike activity and Model 2 for detecting electroencephalographic seizures. The settings for Model 1 are: Bandpass filtering of 10-48 Hz, 80 ms maximum spike duration, 200ms maximum interevent interval, second derivative value of 20 $\mu V/ms^2$, standard deviation amplitude threshold of 8, maximum event duration of 10000 ms, minimum event duration of 0, maximum number of spikes in cluster of 2000, DC voltage offset of 500μV and normalization duration of 50 mins.

Model 2's settings are as follows: Bandpass filtering of 8-30 Hz, 80 ms maximum spike duration, 2000 ms maximum interevent interval, second derivative value of 5 $\mu V/ms^2$, standard deviation amplitude threshold of 4, maximum event duration of 10000000 ms, minimum event duration of 8000 ms, maximum number of spikes in cluster of 2000, DC voltage offset of 5000 μV and normalization duration of 50 mins.

Single spikes and poly spikes were tallied for each recording session based on the vigilance state in which the event occurred in that particular recording from that animal. In order to normalize and control for unequal amounts of activity and inactivity between animals, the total number of spikes from each vigilance state was divided by the total duration of the vigilance state, represented as number of events per minute.

For electroencephalographic seizure detection, a list of potential seizure events was detected by Model 2 as described above, followed by manual inspection by a trained experimenter to evaluate if the seizure event was a true positive or false positive. The experimenter was blinded to the genotype and injection type of the animal.

Statistical analysis

Statistical analysis was performed in R v.4.0.5 using RStudio as frontend for development of analysis scripts. A general linear mixed model (GLMM) was fit to the readouts of epileptiform activity. A detailed description of the GLMM can be found in supplementary methods M4.

To determine if the interaction effects were significant, a null model containing all other terms except for the interaction term of interest was compared to the model via log-likelihood. Significant interactions were determined if the null model was significantly different from the threshold (alpha = 0.05). Subsequent post-hoc comparisons using Benjamini-Hochberg FDR for multiple comparisons were generated. The threshold for determination of significance was set at q = 0.05 for the multiple comparisons after correction using Benjamini-Hochberg FDR. All data was plotted using ggplot2 as bar graphs and dots representing individual animal values and error bars representing standard errors.

Results

Single and poly spike events are significantly influenced by the interaction between the Age of the animal, Vigilance state, Genotype-Treatment combination, and Time-post-injection

In order to understand which independent factors may influence the development of single and poly spikes in the animals in this current study, we applied a GLMM to the dependent variables of single and poly spikes as a function of the interaction of the independent variables of Age at which the animal was injected (simply referred to as Age in the model), Time-post-injection, Vigilance state (Active or Inactive), Genotype-treatment combination and Electrode position. Separate linear models were generated for analysis of single and poly spike data. In addition, APP.PS1 and relevant controls were separately analysed from APP-KI animals and their respective controls due to software limitations.

A full model containing the interaction of factors of interest (i.e. Electrode, Age, Vigilance state, Genotype-Treatment, as well as Time post injection, containing all lower-order interactions as well) was constructed and tested against a model lacking the interaction term of interest using log-likelihood.

We report that a significant interaction effect of Age x Vigilance state x Genotype-treatment, (i.e., χ^2 (3), L-ratio = 20.6596 p = 0.0001) for single spikes and an interaction between Age x Vigilance state x Genotype-Treatment x Time post-injection (χ^2 (12), ratio = 29.03705, p-value = 0.0038) for poly spikes.

We also tested the independent factor of the sex of the animal in relation to the epileptiform activity characterized in this study (i.e., single and poly spikes). We report that there was no significant main effect of the sex of the animal and thus, we did not proceed with subsequent analysis that included sex.

While assessing the presence of electroencephalographic seizure activity in this present study, results were inconclusive in determining whether pathology had any clear effect on this readout. This was primarily due to the lack of sufficient samples quantified from either animal cohort at any of the time points recorded. In order to rule out the possibility of having missed seizure events (i.e., false negatives), Model 2 was validated against a separate study involving the administration of Pentylenetetrazol (PTZ), a commonly used pharmacological compound for inducing seizures [26]. This was tested in a separate cohort of 8 APP.PS1 animals and 5 wild-type C576BL/6 animals, with a 30mg/kg dose of PTZ. APP.PS1 animals exhibited seizures that included convulsions and tail-raising behavior, indicative of a seizure with motoric components. Wild-type animals did not exhibit any convulsions or behavioral indications of seizures, and did not exhibit signs of seizures on EEG. A sensitivity and specificity analysis indicated 100% sensitivity and 71.4% specificity, indicating no false negatives. These results suggest that Model 2 was indeed sensitive enough to reliably detect seizures with little to no false negatives.

While we attempted to quantify the number of seizures during the analysis, there were only a few (<10) incidences of seizures aggregated across all time points, animals, genotypes, treatments and ages. This suggests that very few occurrences of EEG seizures were detected across the study, and

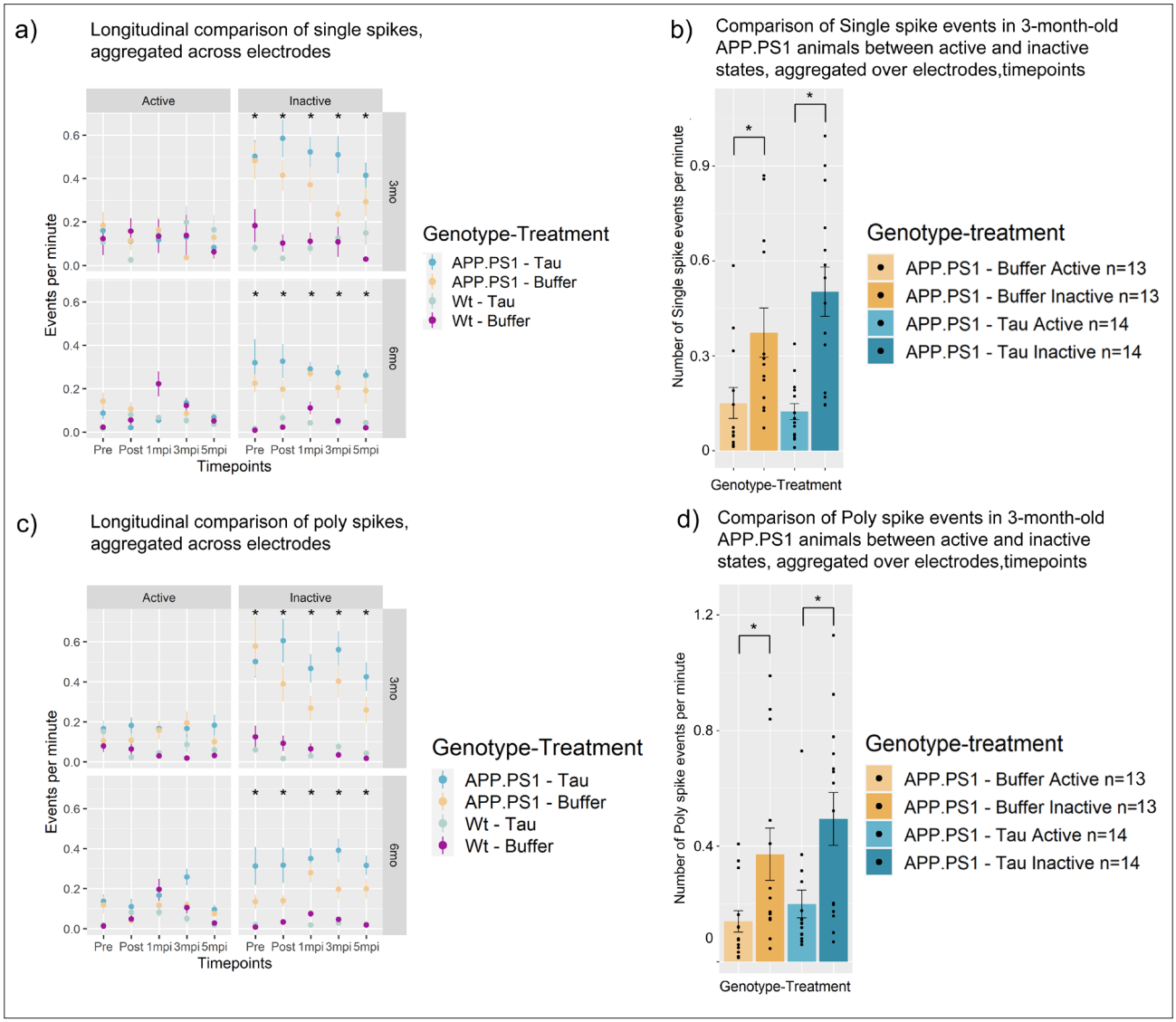


Figure 2: Overview and vigilance state comparison of single and poly spike activity detected in APP.PS1 animals. a) Longitudinal overview of the number of single spike events detected per minute in 3- and 6-month-old APP.PS1 animals in both vigilance states. Asterisks indicate significant differences in means across Genotype-Treatment groups. b) Comparison of single spikes events detected per minute in 3-month-old APP.PS1 animals between active and inactive states. Asterisks indicate significant pairwise comparisons. c) Longitudinal overview of the number of Poly spike events detected per minute in 3- and 6-month-old APP.PS1 animals in both vigilance states. Asterisks indicate significant differences in means across Genotype-Treatment groups. d) Comparison of poly spikes events detected per minute in 3-month-old APP.PS1 animals between active and inactive states. Asterisks indicate significant pairwise comparisons ($p<0.05$). Accompanying p-values for each significant comparison can be found in supplementary table 1.

thus a reliable estimation of significant differences cannot be determined. Due to the detection paradigm used, the small number of EEG seizures detected could have been detected as false positive 'polyspike events', but due to the extremely low number of seizures, it would be highly unlikely to affect the counts of true positive polyspike events. Due to the short daily recording timeframe, one possibility may be that EEG seizures are more prominent during other circadian periods, that could not be detected due to the duration limitations of wireless EEG recordings.

Thus, at the time points and ages used for seizure evaluation, there were insufficient observations to conclude if seizures are influenced by pathology. Other studies have also reported the insufficiency of epileptic seizures in animal models as an obstacle to investigating anti-epileptic treatments [10].

APP.PS1 animals feature significantly elevated levels of single and poly spike activity in states of inactivity compared to control animals at baseline recordings

When we assessed APP.PS1 animals for the presence of single and poly spike activity, we noted that the presence of both single and poly spike phenomena was significantly increased in APP.PS1 animals relative to wild-type controls (Figure 2a).

Notably, single and poly spikes appear to exhibit a preference for periods of inactivity, as seen by significant differences in APP.PS1 animals compared to wild-type animals during inactive states (Figure 2a, 2c) in either age group. When comparing the amount of single and poly spikes, aggregated over time points, electrodes (due to the interaction effect

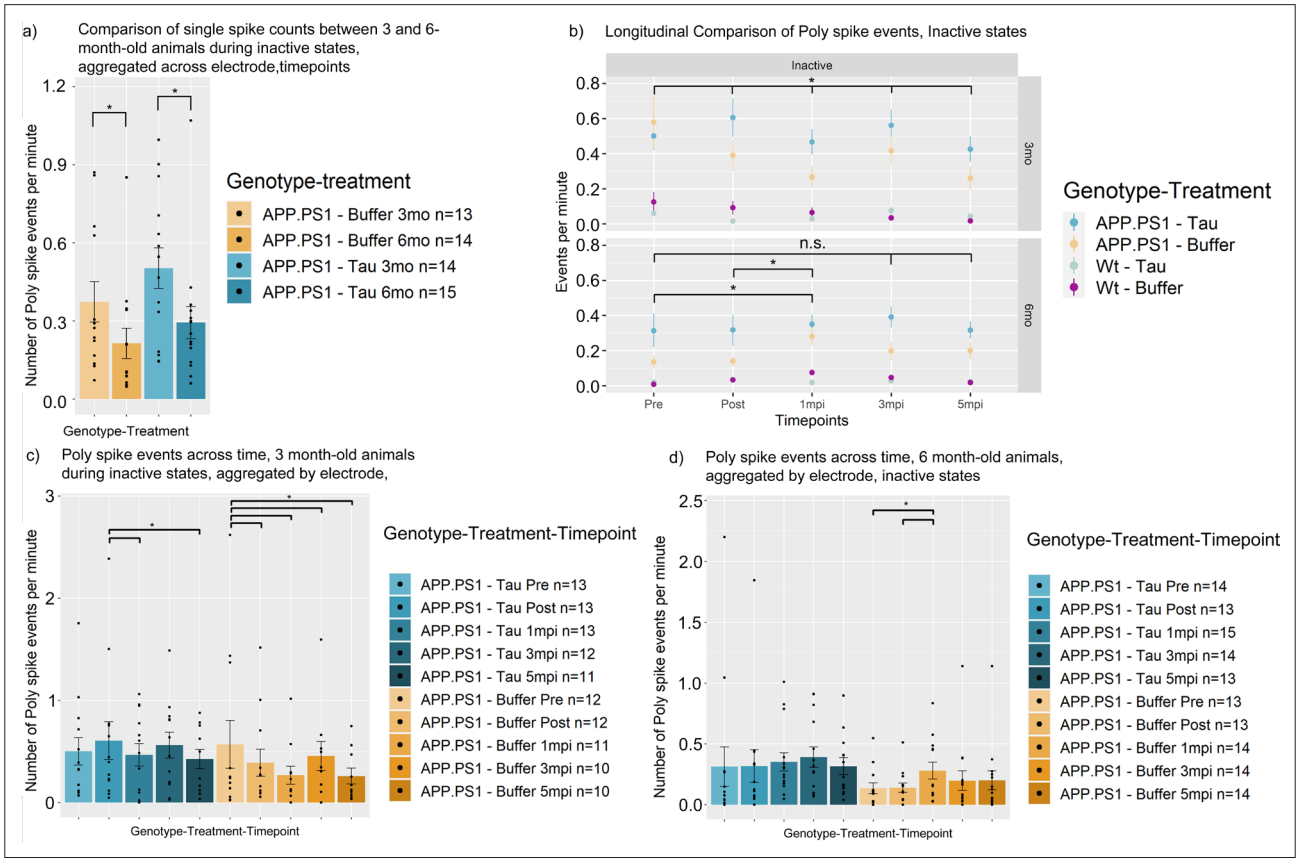


Figure 3: Comparisons across age and time-post-injection in APP.PS1 animals. a) Comparison of single spikes between 3-and 6-month-old animals indicating younger animals exhibit more single spike events compared to older animals. Asterisks indicate significant pairwise comparisons. b) Longitudinal comparison of poly spikes in 3- and 6-month-old-animals demonstrating significant differences in poly spike events from Pre-injection. Asterisks indicate means were significantly different when comparing between respective timepoint and Pre-injection. Comparison of poly spike events illustrating significant pairwise comparisons by Genotype-Treatment groups in c) 3-month-old-animals and d) 6-month-old-animals. Asterisks indicate significance pairwise comparisons ($p<0.05$). Accompanying p-values for each significant comparison can be found in supplementary table 2.

lacking these terms), APP.PS1 animals showcase significantly increased amounts of single spikes (Figure 2a, 2b) and poly spikes (Figure 2c, 2d) in inactive states compared to active states. For more details regarding the pairwise comparisons in figure 2b and 2d, please refer to supplementary table 1c.

In addition, the factor of Genotype-Treatment was present in the interaction effects of single and poly spikes, suggesting that the number of single spikes differ across genotype-treatment groups. Specifically, APP.PS1 animals exhibited significantly more single and poly spike activity compared to their respective wild-type controls (Figure 2a, 2c). For a comprehensive list of all pairwise comparisons of between Genotype-Treatment groups across all recording time points, please refer to supplementary table 1a for single spike events and supplementary table 1b for poly spike events.

These findings indicate that APP.PS1 animals exhibit significant amounts of epileptiform activity compared to wild-type controls, more prominently seen in states of inactivity.

APP.PS1 animals feature an age-dependent decrease in epileptiform activity, which was counteracted by tau seeding

Additionally, the factor of age further complicated the interaction effect, indicating the development of single and poly spike counts differed depending on the age of the animal. Younger APP.PS1 animals demonstrated significantly more single spike activity compared to older animals (Figure 3a, Supplementary Table 2a).

For poly spike activity, there was an interaction effect of time-post injection suggesting that the amount of time after injection also affected this relationship. Thus, we examined this relationship at each time point to understand this. APP.PS1-buffer animals injected at 3 months of age exhibited significant decreases in poly-spike activity between the pre-injection time points and other time points (Figure 3b, 3c, Supplementary Table 2b). In contrast, APP.PS1-tau animals did not exhibit significant differences between pre-injection baselines and other time points, but exhibited a significant difference between post-injection and 1 m.p.i, and post-injection and 5 m.p.i. (Figure 3c, Supplementary Table 2b). In animals injected at 6 months of age, a significant difference was noted between pre-injection and 1 m.p.i, and between pre-injection (Figure 3d, Supplementary Table 2b). For a comprehensive list of all pairwise comparisons of between age groups across all recording time points, please refer to supplementary table 2b for poly spike events.

The significant decline of poly spike activity seen in APP.PS1-buffer animals injected at 3 months of age suggests that epileptiform activity decreases with age in younger animals.

However, the lack of this relationship in APP.PS1-tau animals indicates that tau seeding may prevent age-associated decline of poly spike activity in younger animals.

APP-KI animals exhibited similar interaction effects but completely different single and poly spike profiles

In order to sufficiently address whether the presence of

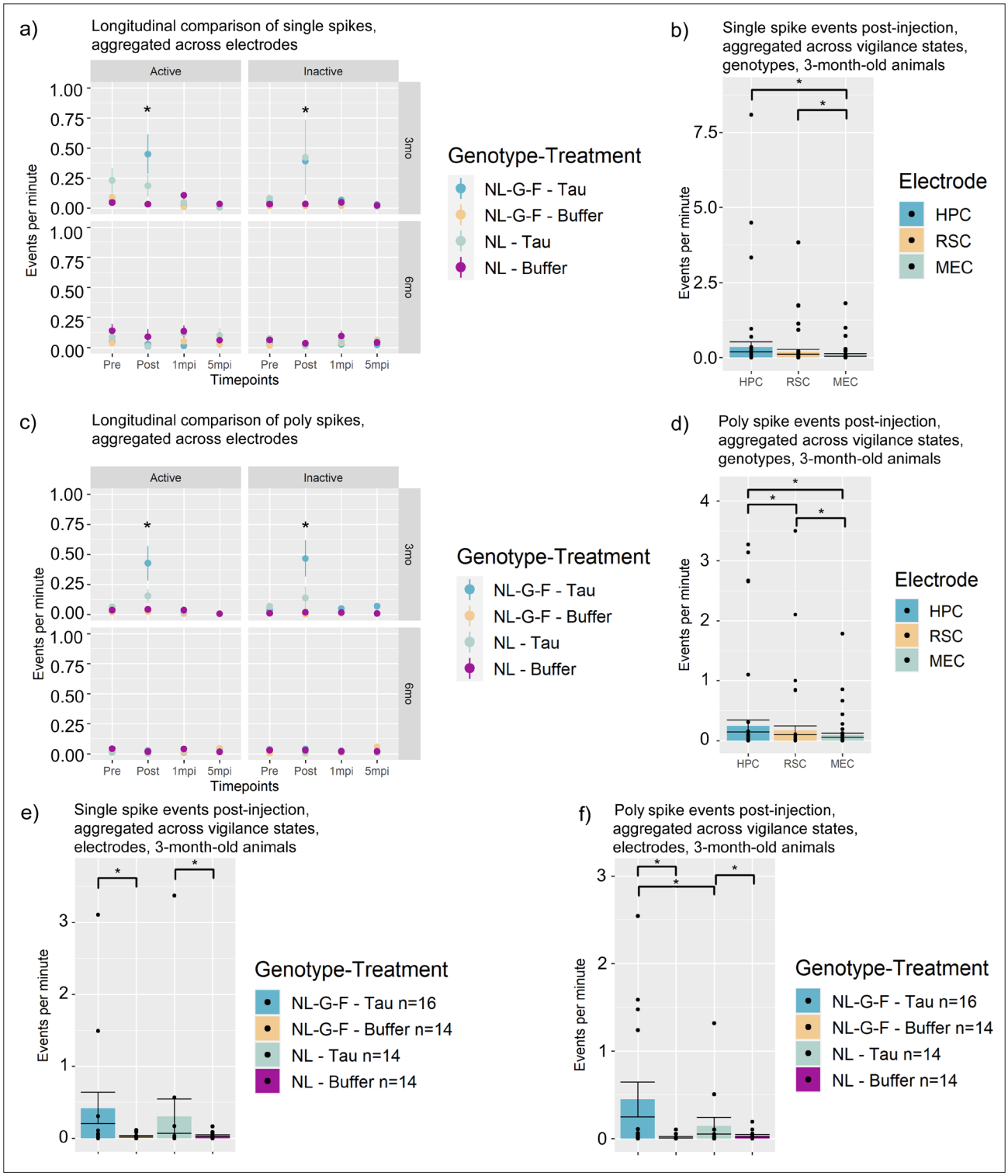


Figure 4: Comparisons of single and poly spike events in APP-KI animals. a) Longitudinal overview of single spike events per minute detected in APP-KI animals across active and inactive states, in 3-and 6-month-old animals. Asterisks indicate means are significantly different at the respective timepoints. b) Single spike events detected across hippocampal (HPC), retrosplenial cortex (RSC) and medial entorhinal cortex (MEC) electrodes. Asterisks denote significant pairwise comparisons. c) Longitudinal overview of poly spike counts per minute in APP-KI animals. Asterisks indicate means are significantly different at the respective timepoints. d) Poly spike counts across individual electrodes demonstrating significantly more poly spike events in the hippocampus compared to other electrodes. Epileptiform activity counts in 3-month old animals immediately after seeding, demonstrating significant increases in e) single spike and f) poly spike counts.

epileptiform activity could be directly attributed to amyloid or tau pathology, the same analysis was performed in APP-KI animals, using the same spike detection model applied to APP.PS1 animals for single and poly spike detection.

Similar to the previous section, the counts of single and poly were tallied for each animal and analysed using a GLMM for determining which factors may interact and contribute to the presence of single and poly spike activity.

We report that an interaction between Age x Genotype-Treatment x Time-post-injection (i.e., χ^2 (12), L-ratio = 29.3574 p-value = 0.0005), Electrode x Age x Time-post-injection (i.e., χ^2 (8), L-ratio = 18.8494 p-value = 0.0044) for single spikes and Age x Genotype-Treatment x Time-post-injection (i.e., χ^2 (12), L-ratio = 81.8132, p-value = 7.05e-14), and Electrode x Age x Time-post-injection (χ^2 (8), L-ratio = 18.06508 p-value = 0.0207 for poly spikes. The interaction effect of Age x Genotype-treatment and Time post injection is similar to the interaction effect in APP.PS1 animals. However, the presence of the Electrode x Age x Time-post-injection was not previously noted in APP.PS1 animals, suggesting that the amount of single and poly spikes differ according to the electrode. These interactions are explored in further details below.

Tau seeding results in acute localized increases in epileptiform activity immediately following seeding

At a cursory examination of single and poly spike counts across Genotype-Treatment groups and time aggregated across electrodes (Figure 4a, 4c), the most salient observation was the increased amount of single and poly spike counts at the post-injection timepoint. This was noted to be present significantly in 3-month-old animals but not 6-month-old animals, which is reflected by the Age factor in the interaction effect. However, apart from the post-injection time point, there are no clear indications of any differences in single or poly spike counts between treatment and genotype conditions.

Due to the factor of Electrode being present, a more detailed investigation on the level of individual electrodes was carried out. This revealed that the hippocampal and retrosplenial cortex electrodes exhibited significantly more single spikes detected compared to the medial entorhinal cortex electrode (Figure 4b). In terms of poly spikes, the hippocampus exhibited significantly increased poly spikes compared to the retrosplenial cortex and entorhinal cortex electrodes (Figure 4d). In addition, the retrosplenial cortex electrode exhibited significantly more poly spikes than the medial entorhinal cortex electrode (Figure 4d). For a detailed list of pairwise comparisons, refer to supplementary table 2c. This suggests that the site of injection (i.e., the hippocampus) exhibited more epileptiform activity following seeding, indicating that tau seeding results in the localized development of epileptiform activity.

The Genotype-Treatment factor also indicated an effect associated with either the Genotype or Treatment, and was further investigated. Both NL-G-F-tau and NL-Tau animals exhibited significantly more single (Figure 4e) and poly spikes (Figure 4f) compared to their respective buffer controls. This result indicates that the injection of tau seeding increases the amount of single and poly spike activity in APP-KI animals. For a detailed list of pairwise comparisons between Genotype-Treatment groups, refer to supplementary table 2d.

Lastly, NL-G-F-tau animals also exhibited more poly spike activity compared to NL-tau animals (Figure 4f), indicating that seeding may be affecting NL-G-F and NL-tau mice differentially, which could be related to the presence of amyloid plaque pathology in NL-G-F animals and not in NL-NL animals. This relationship was not noted for single spike activity, indicating a mechanism related to poly spike activity.

Thus, these findings indicate that the immediate effects of tau seeding are associated with increased epileptiform discharges in APP-KI animals, and is localized to the site of seeding. Furthermore, the effects of poly spike events were significantly higher in NL-G-F animals compared to NL-NL animals, suggesting that amyloid pathology may be slightly affecting this relationship.

Discussion

In this present study, we aimed to answer 2 main questions associated with the presence of epileptiform activity in animal models of AD pathology. The first question pertains to whether the presence of epileptiform activity may be attributable to the presence of pathology in these animals. The investigation of single and poly spikes in APP.PS1 animals revealed that single and poly spikes were abundantly present in states of inactivity, and more so in younger APP.PS1 animals. However, the subsequent investigation in APP-KI animals using the same detection parameters, experimental conditions, ages, time points and treatment conditions revealed a lack of similar levels of single and poly spike activity in APP-KI animals. When comparing amyloid-positive (NL-G-F animals) and amyloid-negative (NL animals) APP-KI animals, no significant differences in either single or poly spikes were noted, except immediately after seeding. This finding indicates that the presence of amyloid plaque pathology may not sufficiently explain the presence of single and poly spike pathology. Thus, this leads to the question of what may be contributing to the presence of epileptiform activity in APP.PS1 animals.

Prior to exploring which factors could be contributing to the presence of increased power spectra and epileptiform activity, it bears noting that there is one crucial genotypic element that distinguishes APP.PS1 animals from APP-KI animals, which is the presence of the presenilin mutation in APP.PS1 animals. The presenilin protein, encoded by the PSEN1 gene is part of the gamma-secretase catalytic complex that controls the cleavage of the APP protein, forming β-amyloid (Aβ) peptides of varying lengths [27]. Mutations in the PS1 gene have been associated with neurophysiological changes in terms of LTP [28, 29]. In addition, numerous mutations on the PS1 gene have been associated with the presence of seizures [30]. Thus, it may also be possible that the presence of PS1 mutations may be in part responsible for the NH phenomena observed in APP.PS1 animals but not APP-KI animals. Recent developments in model development have resulted in APP-KI mouse models with the PSEN1 mutation, and could allow for disentangling the contribution of PSEN1 mutations on the generation of epileptiform activity [31].

The other possibility lies in the fact that the overexpression of APP by itself may be a large factor influencing the presence of epileptiform activity in these animals. One particular study that provides evidence that supports the idea that protein overexpression is associated with aspects of NH, is a study characterizing the effects of overexpressing wild-type human APP [15]. This study noted resulted in several changes, such as cognitive impairment, neuronal loss, and neuronal overexcitation and increased LTP, in the presence of low amounts of amyloid-beta. In addition, the presence of GABAergic deficits was suggested to underlie the presence of overexcitation in this animal models. GABA is a main player mediating the excitatory-inhibitory balance of neural circuits, with several types of epilepsies associated with GABAergic deficits [32, 33], and could explain the presence of the epileptiform activity seen in APP.PS1 animals. Another study also has reported several changes associated with synapse-associated proteins such as PSD95, and glutamate receptors that may render the neuronal network more prone to imbalances in excitation and inhibition [14].

Given that protein overexpression in APP.PS1 animals would also likely result in much higher levels of Aβ40 and Aβ42 fragments than APP-KI animals, it may be possible that these soluble fragments may contribute to epileptiform activity. However, this proposition is unlikely since the fact that NL-G-F animals and NL-NL animals fail to show any significant difference in terms of single and poly spike counts except after seeding, given the gene-dose-dependent increase in soluble species of Aβ40 and Aβ42 [16, 34]. The findings in this study also complement the work done by [13], which noted that genetic suppression of APP was more effective at reducing epileptiform activity instead of reducing soluble species of amyloid. Studies investigating the presence of epileptiform activity in APP-KI animals have reported differing results [4, 11], whereas other studies have reported a lack of difference in other neurophysiological properties indirectly associated with epileptiform activity such as power spectra [22, 35, 36].

However, this also provokes a separate and perhaps, even more fundamental question: If the neurophysiological changes are unrelated to pathology, should they even be investigated further? While overexpression of APP in animal models is arguably not representative of sporadic cases or even familial cases of AD, it may still be of use in modelling patient populations that are associated with increased copies of APP [37, 38], which also exhibit increased risks for seizures. In addition, cases of trisomy 21 or also known as Down's Syndrome (DS) also features an additional copy of APP, as well as increased levels of seizures in DS patients with dementia [39]. Thus, while animal models with protein overexpression may be limited in terms of generalizing to the general AD population, they may still be of use in modeling a more specific population of patients.

The second question this study aimed to answer was if the act of tau seeding, and subsequent development of both amyloid and tau pathology would be associated with the presence of epileptiform activity. APP.PS1-tau animals showed an effect of the injection of tau seeding, which appeared to prevent the age-related decline of epileptiform activity. However, a completely different effect was noted in APP-KI animals, with the injection only resulting in an acute increase in epileptiform activity immediately following injection and no clear indication of any longitudinal effects. In addition, our findings are in line with reports of tau pathology (at least in the form of AT8-positive tau pathology) not significantly affecting the development of seizure activity [40, 41]. However, our present study did not investigate the relationship between tau seeding and PTZ-induced seizures as described in Van Erum et al. Nonetheless, it appears that the presence of tau pathology in the form of AT8-positive tau pathology does not appear to elicit any significant effect on the presence of single and poly spike epileptiform activity in APP-KI animals, even after 5 months post-injection.

One potentially interesting relationship resulting from tau seeding injections is that there may be hints of NH present, particularly in younger APP-KI animals. When comparing the presence of single and poly spikes in APP.PS1 and wild-type animals, wild-type animals did not show any significant increase in single and poly spike activity in either age group after seeding. In contrast, both types of APP-KI animals exhibited significant increases in single and poly spike activity following tau injections, in younger animals. This suggests that APP-KI animals may be nearer to an epileptiform activity threshold compared to wild-type animals for the development of subclinical epileptiform activity such as single and poly spikes. The mechanisms underlying why tau seeding elicits epileptiform activity is still unknown and further investigation needs to be performed, perhaps in the form of a seizurogenic insult such as PTZ or pilocarpine. One possible candidate is neuroinflammation-driven seizures [42], which has been shown to be associated with increased seizure susceptibility following a neuroinflammatory challenge using lipopolysaccharides in rats and mice [43, 44]. The process of seeding tau is likely to induce the activation of microglia, which may manifest in a neuroinflammatory response following seeding [45]. Furthermore, the significantly increased levels of single and poly spikes in the hippocampal electrode, suggests a more focal nature associated with the location of the tau seeding.

Furthermore, this relationship is further complicated by the differential effect of age, which showed that in both APP.PS1 and APP-KI animals, older animals appear less susceptible to epileptiform discharges, and highlights the additional level of complexity associated with determining factors that contribute to the presence of epileptiform activity. Younger APP.PS1 animals exhibited significantly more single spike activity and younger APP-KI animals feature significantly more single and poly spikes following tau seeding. While it is commonly reported that aged animals exhibit more common and severe seizures [46], few studies have focused on the age ranges used in our study, making it harder to understand the processes underlying epileptiform activity in this study. It is known that in clinical studies of epilepsy, children tend to exhibit higher rates of seizure occurrence [47], and this may be similar in the case of younger animals at this range. Thus, the presence of single and poly spike activity being more prevalent in younger animals suggests that studies involving the use of animal models of AD pathology for evaluating epileptiform activity need to consider age as a factor in experimental design.

Conclusions

In conclusion, this present study clearly indicates the disparity of epileptiform activity between APP.PS1 animals and APP-KI animals, which may be attributable to many possible factors, but suggests that APP overexpression may be a strong driver of hyperexcitability. While this suggests that single and poly spikes may be associated with the presence of APP overexpression, it does not preclude the possibility that other forms of epileptiform activity may be present, which were not investigated in this study or at different ages which could be pathology-related instead. In addition, the presence of significant epileptiform activity in APP-KI animals but not wild-type following tau seeding suggests some form of increased susceptibility associated with the amyloidogenic genotype. However, this study contributes to the increasing list of limitations associated with amyloid mouse models that exhibit APP overexpression, and potential confounding effects that could obscure otherwise subtle effects associated with pathology instead.

Ethical Approval

All *in vivo* and *in vitro* studies were performed in strict accordance with the guidelines of the Association for Assessment and Accreditation of Laboratory Animal Care International (AAALAC) and with the European Council Directive of 24 November 1986 (86/609/EEC) and European Ethics Committee directive (2010/63/EU) for the protection of laboratory animals. In line with Belgian governmental directives all protocols were approved by the Animal Care and Use Committee of Janssen Pharmaceutica NV.

Conflicts of Interest

The authors declare that they are working for Janssen Pharmaceutica NV. The authors declare no other commercial or financial relationships that could be construed as a potential conflict of interest.

Funding

This project has received funding from the European Union's Horizon 2020 research and innovation programme under the Marie Skłodowska-Curie actions grant agreement no. 765549, project 'M-GATE'.

Author Contributions

S.T, W.D conceived and designed the in vivo and ex vivo research experiments. S.T. carried out the in vivo and ex vivo experiments, as well as the analysis of in vivo data. D.C provided data analysis support and software support (MATLAB and LabView) for analysis. W.D. provided feedback to shape the manuscript. S.T. wrote the manuscript with input from all authors.

Acknowledgements

We would like to greatly thank Virginia M.Y. Lee and John Q. Trojanowski for providing the human brain samples that were used for the preparation of the AD-tau seeds in this experiment. We thank Magda Smyk, who provided critical input during the development of the manuscript. We would like to thank Kristof van Kolen who produced and provided the antibodies used in the in vitro portion of the experiment. We would also like to thank Heidi Huysmans, Ria Biermans, Sofie Embrechts and Magda Smyk for assisting with electrophysiological recordings. We thank Oyelami Tutu and Abdel Ahnaou for providing the APP.PS1 dataset for validation of the scoring model. We also thank Herve Maurin, Charlotte Delay, Diederik Moechars, Louis De Muynck, Arjan Buist, Jonas Mariën, for their support related to the seeding material. We thank Wim van Der Elst for the statistical support in the analysis of this dataset. We thank Nikolay Manyakov for discussion relating to the datasets obtained.

References

1. Vossel KA, Tartaglia MC, Nygaard HB, Zeman AZ, Miller BL. 2017. Epileptic activity in Alzheimer's disease: causes and clinical relevance. *Lancet Neurol* 16(4): 311-322. https://doi.org/10.1016/S1474-4422(17)30044-3
2. Lam AD, Sarkis RA, Pellerin KR, Jing J, Dworetzky BA, et al. 2020. Association of epileptiform abnormalities and seizures in Alzheimer disease. *Neurology* 95(16): e2259–e2270. https://doi.org/10.1212/WNL.0000000000010612
3. Horváth A, Szucs A, Barcs G, Noebels JL, Kamondi A. 2016. Epileptic seizures in alzheimer disease: a review. *Alzheimer Dis Assoc Disord* 30(2): 186-192. https://doi.org/10.1097/WAD.0000000000000134
4. Brown R, Lam AD, Gonzalez-Sulser A, Ying A, Jones M, et al. 2018. Circadian and brain state modulation of network hyperexcitability in Alzheimer's disease. *eNeuro* 5(2): ENEURO.0426-17. https://doi.org/10.1523/ENEURO.0426-17.2018
5. Tok S, Ahnaou A, Drinkenburg W. 2021. Functional neurophysiological biomarkers of early-stage alzheimer's disease: a perspective of network hyperexcitability in disease progression. *J Alzheimers Dis* 88(3): 809-836. https://doi.org/10.3233/JAD-210397
6. Toniolo S, Sen A, Husain M. 2020. Modulation of brain hyperexcitability: potential new therapeutic approaches in Alzheimer's disease. *Int J Mol Sci* 21(23): 9318. https://doi.org/10.3390/ijms21239318
7. Minkeviciene R, Rheims S, Dobszay MB, Zilberter M, Hartikainen J, et al. 2009. Amyloid β-induced neuronal hyperexcitability triggers progressive epilepsy. *J Neurosci* 29(11): 3453-3462. https://doi.org/10.1523/JNEUROSCI.5215-08.2009
8. Reyes-Marin KE, Nuñez A. 2017. Seizure susceptibility in the APP/PS1 mouse model of Alzheimer's disease and relationship with amyloid β plaques. *Brain Res* 1677: 93-100. https://doi.org/10.1016/j.brainres.2017.09.026
9. Kazim SF, Chuang SC, Zhao W, Wong RKS, Bianchi R, et al. 2017. Early-onset network hyperexcitability in presymptomatic alzheimer's disease transgenic mice is suppressed by passive immunization with anti-human APP/Aβ antibody and by mGluR5 blockade. *Front Aging Neurosci* 9: 71. https://doi.org/10.3389/fnagi.2017.00071
10. Gureviciene I, Ishchenko I, Ziyatdinova S, Jin N, Lipponen A, et al. 2019. Characterization of epileptic spiking associated with brain amyloidosis in APP/PS1 mice. *Front Neurol* 10: 1151. https://doi.org/10.3389/fneur.2019.01151
11. Johnson ECB, Ho K, Yu GQ, Das M, Sanchez PE, et al. 2020. Behavioral and neural network abnormalities in human APP transgenic mice resemble those of App knock-in mice and are modulated by familial Alzheimer's disease mutations but not by inhibition of BACE1. *Mol Neurodegener* 15(1): 53. https://doi.org/10.1186/s13024-020-00393-5

12. Kam K, Duffy ÁM, Moretto J, LaFrancois JJ, Scharfman HE. 2016. Interictal spikes during sleep are an early defect in the Tg2576 mouse model of β-amyloid neuropathology. *Sci Rep* 6: 20119. https://doi.org/10.1038/srep20119
13. Born HA, Kim JY, Savjani RR, Das P, Dabaghian YA, et al. 2014. Genetic Suppression of transgenic APP rescues Hypersynchronous network activity in a mouse model of Alzeimer's disease. *J Neurosci* 34(11): 3826-3840. https://doi.org/10.1523/JNEUROSCI.5171-13.2014
14. Simón AM, Schiapparelli L, Salazar-Colocho P, Cuadrado-Tejedor M, Escribano L, et al. 2009. Overexpression of wild-type human APP in mice causes cognitive deficits and pathological features unrelated to Aβ levels. *Neurobiol Dis* 33(3): 369-378. https://doi.org/10.1016/j.nbd.2008.11.005
15. Kreis A, Desloovere J, Suelves N, Pierrot N, Yerna X, et al. 2021. Overexpression of wild-type human amyloid precursor protein alters GABAergic transmission. *Sci Rep* 11: 17600. https://doi.org/10.1038/s41598-021-97144-3
16. Saito T, Matsuba Y, Mihira N, Takano J, Nilsson P, et al. 2014. Single App knock-in mouse models of Alzheimer's disease. *Nat Neurosci* 17(5): 661-663. https://doi.org/10.1038/nn.3697
17. Tok S, Maurin H, Delay C, Crauwels D, Manyakov NV, et al. 2022. Neurophysiological effects of human-derived pathological tau conformers in the APPKM670/671NL.PS1/L166P amyloid mouse model of Alzheimer's disease. *Sci Rep* 12(1): 7784. https://doi.org/10.1038/s41598-022-11582-1
18. Tok S, Maurin H, Delay C, Crauwels D, Manyakov NV, et al. 2022. Pathological and neurophysiological outcomes of seeding human-derived tau pathology in the APP-KI NL-G-F and NL-NL mouse models of Alzheimer's disease. *Acta Neuropathol Commun* 10(2): 92. https://doi.org/10.1186/s40478-022-01393-w
19. Hirsch LJ, Fong MWK, Leitinger M, LaRoche SM, Beniczky S, et al. 2021. American clinical neurophysiology society's standardized critical care EEG terminology: 2021 version. *J Clin Neurophysiol* 38(1): 1-29. https://doi.org/10.1097/WNP.0000000000000806
20. Kane N, Acharya J, Beniczky S, Caboclo L, Finnigan S, et al. 2017. A revised glossary of terms most commonly used by clinical electroencephalographers and updated proposal for the report format of the EEG findings. revision 2017. *Clin Neurophysiol Pract* 2: 170-185. https://doi.org/10.1016/j.cnp.2017.07.002
21. Radde R, Bolmont T, Kaeser SA, Coomaraswamy J, Lindau D, et al. 2006. Aβ42-driven cerebral amyloidosis in transgenic mice reveals early and robust pathology. *EMBO Rep* 7(9): 940-946. https://doi.org/10.1038/sj.embor.7400784
22. Jacob S, Davies G, De Bock M, Hermans B, Wintmolders C, et al. 2019. Neural oscillations during cognitive processes in an App knock-in mouse model of Alzheimer's disease pathology. *Sci Rep* 9(1): 16363. https://doi.org/10.1038/s41598-019-51928-w
23. Guo JL, Narasimhan S, Changolkar L, He Z, Stieber A, et al. 2016. Unique pathological tau conformers from Alzheimer's brains transmit tau pathology in nontransgenic mice. *J Exp Med* 213(12): 2635-2654. https://doi.org/10.1084/jem.20160833
24. Mathis A, Mamidanna P, Cury KM, Abe T, Murthy VN, et al. 2018. DeepLabCut: markerless pose estimation of user-defined body parts with deep learning. *Nat Neurosci* 21: 1281-1289. https://doi.org/10.1038/s41593-018-0209-y
25. Jin N, Babiloni C, Drinkenburg WH, Hajós M, Nygaard HB, et al. 2021. Recommendations for preclinical testing of treatments against alzheimer's disease-related epileptiform spikes in transgenic rodent models. *J Alzheimers Dis* 88(3): 849-865. https://doi.org/10.3233/JAD-210209
26. White HS, Brown SD, Woodhead JH, Skeen GA, Wolf HH. 1997. Topiramate enhances GABA-mediated chloride flux and GABA-evoked chloride currents in murine brain neurons and increases seizure threshold. *Epilepsy Res* 28(3): 167-179. https://doi.org/10.1016/s0920-1211(97)00045-4
27. Kelleher RJ, Shen J. 2017. Presenilin-1 mutations and Alzheimer's disease. *Proc Natl Acad Sci U S A* 114(4): 629-631. https://doi.org/10.1073/pnas.1619574114
28. Auffret A, Gautheron V, Mattson MP, Mariani J, Rovira C. 2010. Progressive age-related impairment of the late long-term potentiation in Alzheimer's disease presenilin-1 mutant knock-in mice. *J Alzheimers Dis* 19(3): 1021-1033. https://doi.org/10.3233/JAD-2010-1302
29. Dewachter I, Ris L, Croes S, Borghgraef P, Devijver H, et al. 2008. Modulation of synaptic plasticity and Tau phosphorylation by wild-type and mutant presenilin1. *Neurobiol Aging* 29(5): 639-652. https://doi.org/10.1016/j.neurobiolaging.2006.11.019
30. Larner AJ, Doran M. 2006. Clinical phenotypic heterogeneity of Alzheimer's disease associated with mutations of the presenilin–1 gene. *J Neurol* 253(2): 139-158. https://doi.org/10.1007/s00415-005-0019-5
31. Sato K, Watamura N, Fujioka R, Mihira N, Sekiguchi M, et al. 2021. A third-generation mouse model of Alzheimer's disease shows early and increased cored plaque pathology composed of wild-type human amyloid β peptide. *J Biol Chem* 297(3): 101004. https://doi.org/10.1016/j.jbc.2021.101004
32. Kumar SS, Buckmaster PS. 2006. Hyperexcitability, interneurons, and loss of gabaergic synapses in entorhinal cortex in a model of temporal lobe epilepsy. *J Neurosci* 26(11): 4613-4623. https://doi.org/10.1523/JNEUROSCI.0064-06.2006
33. Magloire V, Mercier MS, Kullmann DM, Pavlov I. 2018. Gabaergic interneurons in seizures: investigating causality with optogenetics. *Neuroscientist* 25(4): 344-358. https://doi.org/10.1177/1073858418805002
34. Latif-Hernandez A, Sabanov V, Ahmed T, Craessaerts K, Saito T, et al. 2020. The two faces of synaptic failure in AppNL-G-F knock-in mice. *Alzheimers Res Ther* 12(1): 100. https://doi.org/10.1186/s13195-020-00667-6
35. Jun H, Bramian A, Soma S, Saito T, Saido TC, et al. 2020. Disrupted place cell remapping and impaired grid cells in a knockin model of alzheimer's disease. *Neuron* 107(6): 1095-1112.e6. https://doi.org/10.1016/j.neuron.2020.06.023
36. Nakazono T, Lam TN, Patel AY, Kitazawa M, Saito T, et al. 2017. Impaired *in vivo* gamma oscillations in the medial entorhinal cortex of knock-in alzheimer model. *Front Syst Neurosci* 11: 48. https://doi.org/10.3389/fnsys.2017.00048
37. Cabrejo L, Guyant-Maréchal L, Laquerrière A, Vercelletto M, De la Fournière F, et al. 2006. Phenotype associated with APP duplication in five families. *Brain* 129(Pt 11): 2966-2976. https://doi.org/10.1093/brain/awl237
38. Sleegers K, Brouwers N, Gijselinck I, Theuns J, Goossens D, et al. 2006. APP duplication is sufficient to cause early onset Alzheimer's dementia with cerebral amyloid angiopathy. *Brain* 129(Pt 11): 2977-2983. https://doi.org/10.1093/brain/awl203
39. Lai F, Williams RS. 1989. A prospective study of alzheimer disease in down syndrome. *Arch Neurol* 46(8): 849-853. https://doi.org/10.1001/archneur.1989.00520440031017
40. Gomez-Murcia V, Sandau U, Ferry B, Parrot S, Laurent C, et al. 2020. Hyperexcitability and seizures in the THY-Tau22 mouse model of tauopathy. *Neurobiol Aging* 94: 265-270. https://doi.org/10.1016/j.neurobiolaging.2020.06.004
41. Van Erum J, Valkenburg F, Van Dam D, De Deyn PP. 2020. Pentylenetetrazole-induced seizure susceptibility in the tau58/4 transgenic mouse model of tauopathy. *Neuroscience* 425: 112-122. https://doi.org/10.1016/j.neuroscience.2019.11.007
42. Pracucci E, Pillai V, Lamers D, Parra R, Landi S. 2021. Neuroinflammation: a signature or a cause of epilepsy? *Int J Mol Sci* 22(13): 6981. https://doi.org/10.3390/ijms22136981
43. Kovács Z, Dobolyi A, Juhász G, Kékesi KA. 2014. Lipopolysaccharide induced increase in seizure activity in two animal models of absence epilepsy WAG/Rij and GAERS rats and Long Evans rats. *Brain Res Bull* 104: 7-18. https://doi.org/10.1016/j.brainresbull.2014.03.003

44. Sayyah M, Javad-Pour M, Ghazi-Khansari M. 2003. The bacterial endotoxin lipopolysaccharide enhances seizure susceptibility in mice: involvement of proinflammatory factors: nitric oxide and prostaglandins. *Neuroscience* 122(4): 1073-1080. https://doi.org/10.1016/j.neuroscience.2003.08.043

45. Morales I, Jiménez JM, Mancilla M, Maccioni RB. 2013. Tau oligomers and fibrils induce activation of microglial cells. *J Alzheimers Dis* 37(4): 849-856. https://doi.org/10.3233/JAD-131843

46. Kelly KM. 2010. Aging models of acute seizures and epilepsy. *Epilepsy Curr* 10(1): 15-20. https://doi.org/10.1111/j.1535-7511.2009.01341.x

47. So EL. 2010. Interictal epileptiform discharges in persons without a history of seizures: what do they mean? *J Clin Neurophysiol* 27(4): 229-238. https://doi.org/10.1097/WNP.0b013e3181ea42a4